Communications on Applied Nonlinear Analysis
ISSN: 1074-133X
Vol 32 No. 6s (2025)

Superior Asymmetrical PWM AC Chopper Fed Capacitor Run Induction Motor Drive using Evaporation Based Water Cycle Algorithm

Murali Narayanamurthy[1], Annamalai Muthu[2], Gobi Mohan Sivasubramanian[3], Vidhya Prakash Rajendran[4]

[1,2,3,4]Lecturer, College of Engineering & Technology, University of Technology and Applied Sciences-Nizwa
murali.naryanamurthy@utas.edu.om

Article History:

Received: *22-10-2024*

Revised: *06-12-2024*

Accepted: *15-12-2024*

Abstract:

Introduction: This research presents a novel improved asymmetric pulse width modulation technique for increasing the efficiency of a capacitor-powered, pulse width modulated (PWM) AC chopper-supplied induction motor. It uses a water cycle optimization technique based on evaporation and incorporates 4 distinct pulses in each quarter cycle. It is compared with the standard method of sinusoidal pulse-width modulation. Power quality is defined by properties such as input power factor, efficiency, and total harmonic dispersion of voltage and current. Simulation results yields better response for the proposed method when compared with the conventional technique.

Objectives: The goal of the study is to minimize total harmonic distortion of voltage and total harmonic distortion of current while optimizing power factor and efficiency in order to improve power quality metrics. This paper focuses on obtaining the optimal switching angles by an evaporation-based water cycle algorithm.

Methods: The pulses in the enhanced asymmetrical pulse width modulation approach have varying widths while maintaining quarter cycle symmetry. The switching on angles and switching off angles is varied. The proposed enhanced asymmetrical pulse width modulation by evaporation-based water cycle algorithm and conventional sinusoidal pulse width modulation technique is compared.

Results: The simulation results show that performance parameters by proposed technique is better compared to conventional technique. The controlling techniques implemented for PWM AC chopper are sinusoidal pulse width modulation and enhanced asymmetrical pulse width modulation by evaporation based water cycle optimization algorithm.

Conclusions: This paper discusses novel optimization algorithm for the speed control of capacitor run induction motor with improved parameters. The performance enhancement parameters taken into account total harmonic distortion of current, total harmonic distortion of voltage, efficiency and power factor. This work can be compared with the other techniques like particle swarm optimization, cuckoo search optimization and proposed technique for the enhanced asymmetrical pulse width modulation for capacitor run induction motor.

Keywords: Evaporation based water cycle algorithm, Efficiency, Asymmetrical pulses, Switching angles

1. Introduction

High power factor during operation is an inherent benefit of the capacitor run induction motor. In industry, fans are used to circulate air within buildings, and speed control is essential. The industrial specifications need high power quality for efficient operation [1]. The power quality parameters are

good power factor above 0.8 and the harmonic distortions should be below 5% as per the IEEE standard [2]. The literature lists several methods for controlling the speed of an ac to ac converter, including integral cycle control, ac voltage controllers, single and other practices followed [3]. Comparing the modern techniques to other methods mentioned in the literature, the former performs better.

The novel ac to ac converter is proposed to minimize the sag and swell problems [4]. Compared to the conventional type the shoot through problem is not possible as both the switches can be turned on [5]. Validation and application of the simulation and experimental results to various industrial applications are done [6]. The teaching learning optimization approach is used by the PWM AC chopper to lower the output voltage's harmonic. The intended output voltage serves as the basis for the objective function, and the switching angles are chosen to minimize total harmonic distortion. The simulation is carried out by PSIM software to validate the result [7].

The multilevel inverter by Taguchi design approach is used to choose the parameters for genetic algorithm for the design of switching angles. The simulation is validated with PSIM software and the result shows that %THD is 15% or more for the odd harmonics and need to reduce to lesser value for better operation [8]. Solar powered induction motor control utilizes the PWM control for reducing the total harmonic distortion of current [9]. The carrier frequency is inversely proportional to the harmonic distortion. The simulation is incorporated using MATLAB and experimental analysis is not included for validating the result [10].

2. Objectives

This article compares the recommended practices, which incorporates a proposed technique, with the traditional controller. Enhancement of recommended practices is a new method of removing output voltage harmonics. For capacitor-run induction motors, various optimization techniques are included to improve performance under various loading scenarios.

For applying the increased asymmetrical pulse width modulation strategies, the literature provides the following methods: whale optimization algorithm, genetic algorithm, meta-heuristic approach, and bacteria foraging optimization [11]. This work is divided into four sections: section 3 controls the induction motor that is run by a capacitor and details the mechanism for the water cycle that relies on evaporation and section 4 contrasts the results of the proposed approach with those of the conventional system. An induction motor with a fixed capacitor has a fixed capacitor for both initial and continuous operation. The main application with the necessary control is required for domestic fans utilized in industry and household applications.

3. Methods

Using a PWM AC chopper, capacitor run induction's performance is improved under sinusoidal pulse width modulation control [12]. A primary IGBT device and a series of combinations with four diodes are used in this topology. Through the main switch S1, the load current passes through both the positive and negative half cycles. Due to the inductive nature of the motor load, adequate freewheeling action is necessary for energy dissipation. Thus, supplemental switch S2 is used to dissipate power throughout the positive half cycle and the negative cycle. It is necessary to generate the triggering signal for both the freewheeling switch and the main switch. During the positive half cycle, electricity passes through

diode D1, switch S1, diode D4, run the induction motor connected to the capacitor, and then return to the supply. The current passes via the capacitor, the induction motor, diode D3, switch S1, diode D2, and the linked supply voltage during the negative half cycle. The freewheeling action travels through the following paths throughout the positive half cycle: load, D3', switch S2, D2', and load again. The motion of freewheeling passes through the load path, D1', switch S2, D4', and back to load during the negative half cycle.

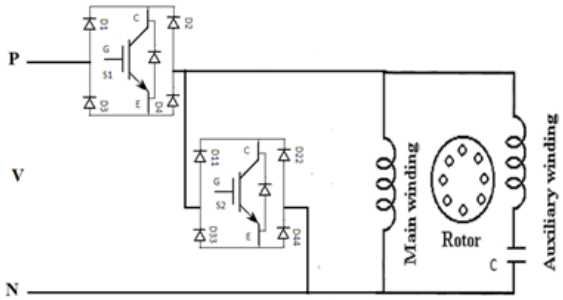

Fig. 1 - Induction motor driven by a capacitor supplied PWM AC chopper.

Pulses in symmetrical pulse width modulation have the same width and preserve full-cycle symmetry [13]. The harmonics in the waveform are mathematically illustrated by the Fourier series; the harmonic frequency component is separated using Fourier transforms [14]. The non-linear harmonic elimination equation can be solved numerically using techniques such as the Newton Raphson method [15]. The solution takes more iteration till it converges to reduced harmonic frequency components. Hence different optimization techniques are evolved for solving these constraint problems [16]. Various techniques, including genetic algorithms, particle swarm optimization, bee colony optimization, and artificial intelligence techniques, are employed in harmonic elimination procedures. Assume that there are N pulses. G1, G2, G3, G4, and H1, H2, H3, H4 are the switching moments that turn the device on or off respectively. The output voltage expressed in the Fourier series is given as

$$V_o = \sqrt{2}V_i\left[Y_o + \sum_{p=1}^{\infty}(Y_p Sin(p\omega t) + Y_p Cos(p\omega t)\right] (1)$$

Where p = 1,2,3…

When all parts are removed, the output voltage can be written as

$$V_o = \sqrt{2}V_i\sum_{p=1}^{\infty}(Y_p Sin(p\omega t)) \quad (2)$$

Where n =1,3,5….

The expression for the fundamental quantity Y1 is

$$Y_1 = \frac{1}{\pi}\sum_{q=1}^{N}\left[H_q - G_q - \frac{Sin2H_q - Cos2G_q}{2}\right] \quad (3)$$

The expression for the Harmonic Quantity Yp is

$$Y_p = \frac{1}{\pi}\sum_{q=1}^{N}\left[\frac{Sin(p-1)H_q - Sin(p-1)G_q}{p-1} - \frac{Sin(p+1)H_q - Sin(p+1)G_q}{p+1}\right] \quad (4)$$

Where p = 3,5,7…

The output voltage and current's total harmonic distortion is provided as [17]

$$THD_V = \frac{\sqrt{\sum_{p=3}^{\infty} V^2_{on}}}{V_1} \quad (5)$$

$$THD_i = \frac{\sqrt{\sum_{p=3}^{\infty} I^2_{on}}}{I_1} \quad (6)$$

A suitable formulation is required to lower the total harmonic distortion at the output. The ideal switching angles provide the pulses required for the ac chopper's improved asymmetrical pulse width modulation. The provided objective function is as follows:

$$\underset{A,B}{Min}\, G = \sqrt{\left[(C_1 - V_{ref})^2 + C_3^{\,2} + C_5^{\,2} + ...C_n^{\,2}\right]} \quad (7)$$

The goal function's constraint is stated [11]

$$0 \le A_1 \le B_1 \le \phi..... \le A_N \le B_N \le B_{\max} \quad (8)$$

A quarter cycle comprises N=4 pulses, Vref is the reference output voltage. Switching instants are turned on and off by A and B. The greatest 90-degree switching angle is known as Bmax. The boundary switching angles are represented by T, and for each set of pulses, the boundary is 22.5 degrees.

The fundamental concept of the evaporation-based water cycle algorithm relies on rivers and streams flowing into the sea as a recurrent process [18]. Assuming a specific location experiences rainfall, the first population of streams is created at random. The sea is chosen as the stream with the lowest objective function and the best value. Directly into rivers or the sea go the other values of streams. The water from the stream is absorbed by the sea or river. The many streams determine how much water is transferred. Stream flow provides a better answer for the minimum objective function than rivers do, and this can be traded for an accurate result [19]. In this sense, the optimal option also involves exchanging the river and the sea. In order to prevent the objective function minimization becoming convergent too soon, the evaporation operator is implemented. Drizzle is produced in streams and rivers by the evaporation process that takes place in the sea [20]. By creating new streams and rivers near the sea, the drizzle ensures the best possible result. Therefore, the stream and river's location is changed to look for. The algorithm steps are discussed below

step 1: Select the Nsr, dmax, Npop, iteration number, and Pareto archive size as the search space's starting parameters.

step 2: Select the starting population size at random for rivers, streams, and seas.

step 3: calculate the objective function for each stream.

step 4: find the answers for the initial random population by storing them in the Pareto archive, then determine the crowding distance to choose the rivers and sea.

step 5: find the flow concentration of rivers and sea by using the governing equations for calculating the crowding values.

$$Obj_n = FF_n - FF_{Nsr+1} \quad n = 1,2,3..., N_{sr} \quad (9)$$

$$NS_n = round\left\{\left|\frac{Obj_n}{\sum_{n=1}^{Nsr} Obj_n}\right| XN_{Streams}\right\} \quad n = 1,2,3..., N_{sr} \quad (10)$$

stage 6: The new position streams may flow directly to the sea, and the associated equation indicates that exchanging the positions of the sea with the stream yields the least objective function.

$$Y_{Stream}^{t+1} = Y_{Stream}^{t} + rand * C * (Y_{Sea}^{t} - Y_{Stream}^{t}) \quad (11)$$

stage 7: The equivalent equation is as follows: the new position streams flow into the rivers and swap the locations of a river with stream to obtain the minimum objective function.

$$Y_{Stream}^{t+1} = Y_{Stream}^{t} + rand * C * (Y_{River}^{t} - Y_{Stream}^{t}) \quad (12)$$

stage 8: The new position river flows into the sea and exchange the locations of the sea with river gives minimum objective function as the corresponding equation is

$$Y_{River}^{t+1} = Y_{River}^{t} + rand * C * (Y_{Sea}^{t} - Y_{River}^{t}) \quad (13)$$

The rand is the random value from zero to one.

stage 9: When the evaporation condition dmax is met, the rainy process begins. Determine the new location with the lowest value by calculating the goal function. The Pareto archive is updated and the higher values are removed.

step 10: Find each Pareto archive's crowding distance and remove the lowest values. Step 6 will be followed if the convergence condition is not met by the newly chosen locations for the rivers and sea.

Table 1 The ideal angles for switching

V0	G1	H1	G2	H2	G3	H3	G4	H4
100	12.03	22.5	25.91	27.14	47.67	57.56	88.65	90
120	12.98	21.48	23.86	33.02	64.37	66.45	87.5	90
140	1.52	20.22	39.91	42.51	48.13	53.95	68.66	90
160	1.87	16.06	32.34	37.94	45.08	67.21	72.18	90
180	9.73	18.41	43.79	44.20	52.06	58.27	75.40	90
200	2.74	17.06	29.82	31.84	57.19	67.34	71.50	90

4. Results

MATLAB software is used to compute the proposed algorithm.

The following is a list of the parameters used.

Population size: 50

Number of rivers and sea: 4

Evaporation condition constant: 1e-5

Maximum number of iterations: 100

Table 2 presents a comparative analysis between the conventional technique, artificial bee colony algorithm-based methodology, and modern technology. It suggests a proposed method for an output voltage of 160V. The goal function's convergence attained after various iterations. There were 100 iterations in the outcome. Figure 2 displays the objective function after it has been decreased to a value of 0.518%. Efficiency, power factor, and total harmonic distortion are the benchmarks for performance improvement.

Table 2 Relative evaluation of several methods

Approach	%THDv	%THDi	Power factor
EEWCA	1.25	0.82	0.93
BCO [5]	16.15	16.15	0.81
SPWM	22.66	11.62	0.83

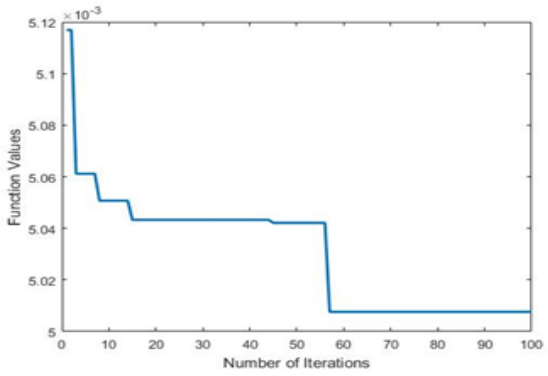

Fig. 2 - Convergence diagram for several repetitions.

5. Discussion

The suggested method has a total harmonic distortion current of 0.77% at 180V, compared to 17.8% for the standard methodology. The suggested algorithmic approach is 17.03% less complex than the traditional method. For the suggested approach, the total harmonic distortion current is within the IEEE standard limit. Figure 3 illustrates how the reduced current harmonic distortion results in the least amount of losses.

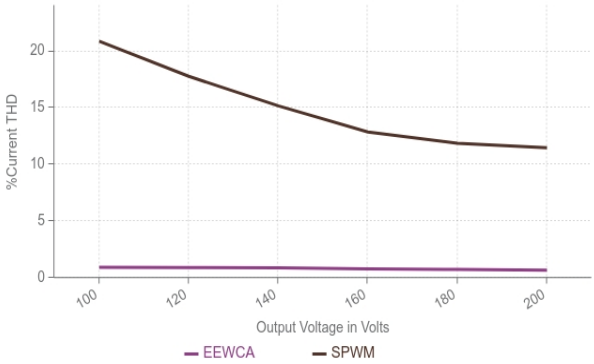

Fig. 3 - %THD current for the suggested method and the traditional one.

The suggested technology has 1.12% overall harmonic distortion voltage at 180V, compared to 20.5% for the conventional method. When compared to the conventional technique, the total harmonic distortion voltage of the suggested technique is 19.38% lower. The total harmonic distortion voltage for the suggested approach, under various loading conditions, is within the IEEE standard limit is shown in figure 4.

Fig. 4 - %THD voltage for proposed and conventional technique.

At 180V, the evaporation-based water cycle algorithm has a efficiency of 76% compared to the sinusoidal pulse width modulation technique of 67%. It infers that the evaporation-based water cycle algorithm technique has 9% more efficiency compared to the sinusoidal pulse width modulation technique. The proposed method is better when compared to the conventional method for the capacitor run induction motor is shown in figure 5.

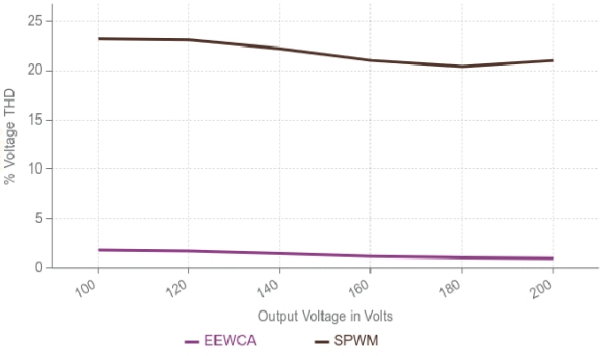

Fig. 5 - %Efficiency for proposed and conventional technique

At 180V, the evaporation-based water cycle algorithm has a power factor of 0.93 compared to the sinusoidal pulse width modulation technique of 0.86. It infers that the evaporation-based water cycle algorithm technique has 0.07 more power factor compared to the sinusoidal pulse width modulation technique. The more power factor leads to distortion less operation of capacitor run induction motor is shown in figure 6.

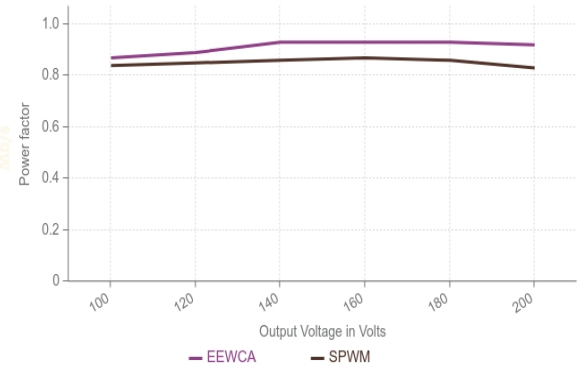

Fig. 6 – Power factor for proposed and conventional technique

References

[1] Wang, Y., Wang, P., Cai, G., Liu, C., Guo, D., Zhang, H., & Zhu, B. (2021). An improved bipolar-type AC–AC converter topology based on nondifferential dual-buck PWM AC choppers. IEEE Transactions on Power Electronics, 36(4), 4052–4065. doi:10.1109/tpel.2020.3022026

[2] Ghorpade, D. B., Koshti, A. S., & Halve, S. S. (2020). Reduction of selective harmonics in PWM AC chopper using teaching–learning-based optimization. In Lecture Notes in Electrical Engineering. Lecture Notes in Electrical Engineering (pp. 229–237). doi:10.1007/978-981-15-0313-9_17

[3] Metwaly, M. K., Azazi, H. Z., Deraz, S. A., Dessouki, M. E., & Zaky, M. S. (2019). Power factor correction of three-phase PWM AC chopper fed induction motor drive system using HBCC technique. IEEE Access: Practical Innovations, Open Solutions, 7, 43438–43452. doi:10.1109/access.2019.2907791

[4] Süleyman, A., Hasan, C. (2021). Analysis of Total Harmonic Distortion of an Induction Motor In Off-Grid PV Systems Depending on Carrier Frequency, 5, 27–40.

[5] Lopez, A. R., Sosa, J. M., Juarez, M. A., Torres, F.-J., & Correa-Betanzo, C. (2020), November 4). Calculation of optimal switching angles for a multilevel inverter through the Taguchi design approach. 2020 IEEE International Autumn Meeting on Power, Electronics and Computing (ROPEC). Presented at the 2020 IEEE International Autumn Meeting on Power, Electronics and Computing (ROPEC), Ixtapa, Mexico. doi:10.1109/ropec50909.2020.9258728

[6] Suwongsa, T., Areerak, K., Areerak, K., & Pakdeeto, J. (2021). Energy saving approach for an electric pump using a fuzzy controller. Energies, 14(11), 3330. doi:10.3390/en14113330

[7] Soliman, M. A., Hasanien, H. M., Al-Durra, A., & Alsaidan, I. (2020). A novel adaptive control method for performance enhancement of grid-connected variable-speed wind generators. IEEE Access: Practical Innovations, Open Solutions, 8, 82617–82629. doi:10.1109/access.2020.2991689

[8] Barzegar, A., Sadollah, A., & Su, R. (2019). A novel fully informed water cycle algorithm for solving optimal power flow problems in electric grids. doi:10.48550/ARXIV.1909.08800

[9] Moradi, M., Sadollah, A., Eskandar, H., & Eskandar, H. (2017). The application of water cycle algorithm to portfolio selection. Economic Research-Ekonomska Istraživanja, 30(1), 1277–1299. doi:10.1080/1331677x.2017.1355254

[10] Yanjun, K., Yadong, M., Weinan, L., Xianxun, W., & Yue, B. (2017, May). An enhanced water cycle algorithm for optimization of multi-reservoir systems. 2017 IEEE/ACIS 16th International Conference on Computer and Information Science (ICIS). Presented at the 2017 IEEE/ACIS 16th International Conference on Computer and Information Science (ICIS), Wuhan, China. doi:10.1109/icis.2017.7960022

[11] Murali, N., & Balaji, V. (2018, July). Enhanced Asymmetrical PWM AC chopper fed capacitor run induction motor drive using Bacterial Foraging Optimization Algorithm. 2018 International Conference on Recent Innovations in Electrical, Electronics & Communication Engineering (ICRIEECE). Presented at the 2018 International Conference on Recent Innovations in Electrical, Electronics & Communication Engineering (ICRIEECE), Bhubaneswar, India. doi:10.1109/icrieece44171.2018.9008661

[12] Hasanien, H. M. (2018). Performance improvement of photovoltaic power systems using an optimal control strategy based on whale optimization algorithm. Electric Power Systems Research, 157, 168–176. doi:10.1016/j.epsr.2017.12.019

[13] Kumar, R., & Sinha, N. (2020). Modeling and control of dish-Stirling solar thermal integrated with PMDC generator optimized by meta-heuristic approach. IEEE Access: Practical Innovations, Open Solutions, 8, 26343–26355. doi:10.1109/access.2020.2970613

[14] Dahidah, M. S. A., & Agelidis, V. G. (2008). Selective harmonic elimination PWM control for cascaded multilevel voltage source converters: A generalized formula. IEEE Transactions on Power Electronics, 23(4), 1620–1630. doi:10.1109/tpel.2008.925179

[15] Metwaly, M. K., Azazi, H. Z., Zaky, M. S., & Deraz, S. A. (2018). Power factor correction of four-switch three-phase inverter-fed sensorless induction motor drives with partial electrical free measurement. Electric Power Components & Systems, 46(7), 837–851. doi:10.1080/15325008.2018.1509912

[16] Azazi, H. Z., Ahmed, S. M., & Lashine, A. E. (2018). Single-stage three-phase boost power factor correction circuit for AC–DC converter. International Journal of Electronics, 105(1), 30–41. doi:10.1080/00207217.2017.1335800

[17] Deraz, S. A., Azazi, H. Z., Zaky, M. S., Metwaly, M. K., & Dessouki, M. E. (2019). Performance investigation of three-phase three-switch direct PWM AC/AC voltage converters. IEEE Access: Practical Innovations, Open Solutions, 7, 1–1. doi:10.1109/access.2019.2892523

[18] Hasanien, H. M., & Matar, M. (2018). Water cycle algorithm-based optimal control strategy for efficient operation of an autonomous microgrid. IET Generation, Transmission and Distribution, 12(21), 5739–5746. doi:10.1049/iet-gtd.2018.5715

[19] El-Fergany, A. A., & Hasanien, H. M. (2019). Water cycle algorithm for optimal overcurrent relays coordination in electric power systems. Soft Computing, 23(23), 12761–12778. doi:10.1007/s00500-019-03826-6

[20] Panfilov, D. I., ElGebaly, A. E., & Astashev, M. G. (2017, October). Design and evaluation of control system for static VAR compensators with thyristors switched reactors. 2017 IEEE 58th International Scientific Conference on Power and Electrical Engineering of Riga Technical University (RTUCON). Presented at the 2017 IEEE 58th International Scientific Conference on Power and Electrical Engineering of Riga Technical University (RTUCON), Riga. doi:10.1109/rtucon.2017.8124782